J-Researchers

Journal of Civil Engineering Researchers

Journal homepage: www.journals-researchers.com

Investigation of the Effect of High Temperature on the Microstructure of Conventional Concrete Containing High Grade of Portland Cement

Mohammadhossein Mansourghanaei,[a,*]

[a] *Department of Civil Engineering, Chalous Branch, Islamic Azad University, Chalous, Iran*

ABSTRACT

In this laboratory study, a mixed concrete design containing 500 kg/m3 Portland cement was prepared, and elastic modulus testing, X-ray diffraction (XRD) analysis, and scanning electron microscope (SEM) image analysis were performed on concrete samples at 21 and 600 °C after a curing age of 90 days to investigate and evaluate the microstructure of concrete at room temperature and under high temperature. The results of the tests indicate that high temperature causes a decrease in the results, so that the elastic modulus of concrete experienced a decrease of 71.63% from 73.33 GPa at 21°C to 24.12 GPa at 600 °C, and in the XRD analysis, a decrease in the height of the peaks of hydrated elements is observed. The low peak height of calcium hydroxide in the XRD spectrum indicates a proper polymerization process in conventional concrete. In SEM analysis, at a temperature of 21 °C, due to the completion of a large part of the polymerization process, the tree structure, pores and unhydrated particles are seen in their minimum amount, but after applying a temperature of 600 °C to the concrete sample, with damage to the microstructure of the concrete and the hydrated calcium aluminum sulfate (C-A-S-H) and hydrated calcium silicate (C-S-H) gels, an increase in the tree structure, pores and cracks is evident in the concrete sample.

ARTICLE INFO

Received: January 12, 2025
Accepted: February 26, 2025

Keywords:
Ordinary Concrete
Heat
Modulus of Elasticity
Hydrated Calcium Silicate (C-S-H)
Calcium Hydroxide (Ca(OH)2)

DOI: 10.61186/JCER.7.1.62
DOR: 20.1001.1.22516530.1399.11.4.1.1

1. Introduction

In order to develop national security and passive defense in the field of civil engineering infrastructure, a lot of laboratory work has been done to produce structural concrete for strategic and sensitive centers of the country [1-3]. The strength of reinforced concrete structures of these centers plays an important role in reducing destruction and human injuries caused by enemy defense operations. Improving the strength of concrete can be achieved through the type of materials used in its mixture composition [4-10].

There are various methods to improve the mechanical properties and durability of ordinary concrete, and these goals can be achieved to some extent by increasing the grade of Portland cement in ordinary concrete. Research has shown that by increasing the grade of cement in concrete and keeping the water-to-cement ratio low, the mechanical properties of concrete can be increased, and the weak performance of concrete in these conditions can be

* Corresponding author. Tel.: +989121712070; e-mail: mhm.ghanaei@gmail.com.

compensated by adding superplasticizers [1,2,11]. In concretes with a low water-to-cement ratio, the appropriate amount of cement causes a higher concentration of the cement paste and a reduction in the existing porosity. After the polymerization process (hydration or polymerization), the pores of the concrete become smaller and, as the polymerization reaction continues, these small pores are also blocked [12]. The grade of cement used in the concrete mixture has a direct effect on the elastic modulus of the concrete [13]. Understanding the microstructure of concrete is a great help in understanding changes in the macrostructure and rheological, physical and durability performance of concrete.

The microstructure of concrete consists of various parts. According to the microstructural studies conducted by Mehta and Monteiro [14], the hydrated cement paste in ordinary concrete containing Portland cement consists of four important parts. The first and main part consists of a hydrated calcium silicate gel called tobermorite gel (C-S-H), which constitutes 50 to 60 percent of the volume of the hydrated paste. The second part consists of calcium hydroxide called portlandite (Ca(OH)2), which constitutes 20 to 25 percent of the volume of the hydrated cement paste. This compound plays a reactive role in combination with other cementitious materials in the polymerization process. In well-hydrated concretes, the presence of this compound reaches its minimum level. The third part is the hydrated calcium aluminosulfate gel, known as ettringite gel (C-A-S-H), and the fourth part belongs to the unhydrated clinker grains and other components that did not participate in the polymerization process. According to the definition, the C-S-H gel with a variable chemical formula and amorphous structure constitutes a large part [14,15] of the volume of hydrated cement paste and is the main reason for the mechanical properties and durability of hardened concrete [16,17]. However, studies have shown that the hydrated calcium aluminosulfate gel has a weakness in the vicinity of sulfate environments and Ca(OH)2 crystals have a weakness in the vicinity of acidic environments, so the presence of these compounds in concrete will play a significant role in reducing the durability properties of concrete.

The size of C-S-H gel has been estimated to be in the range of 14 angstroms [17]. Richardson has classified the structure of C-S-H gel into four types: tobermorite, japhite, zenite and metagenite, which follow the pseudo-tobermorite model, zenite having a higher calcium to silica (Ca/Si) ratio than tobermorite (which has a ratio of 1.5) [17]. The structure of zenite was first proposed by Taylor in 1968 [18]. This researcher obtained metagenite by heating zenite in the temperature range of 70–90 °C and developed the metagenite model to japhite. C-S-H gel constitutes the largest volume of hydrated cement paste in ordinary concrete. The main product of hydrated cement paste in conventional concrete with a calcium to silica (Ca/Si) ratio of 1.5 to 2 is C-S-H gel, which has a tobermorite or zenite-like structure [17]. The C-S-H structure may be based on tobermorite or zenite, so the C-S-H structure in one part of the hydrated cement paste may be different from another part of the paste. One of the reasons for this is the changes in the calcium to silica (Ca/Si) ratio at different points in the mixture, which leads to morphological changes in the C-S-H structure, which is effective in changing the density and porosity of the tobermorite gel [19]. Figure 1 shows a diagram of the direct model of the C-S-H gel structure, where P is represented by silicate tetrahedra at the O-O edges connected to the central Ca-O layer (paired tetrahedra) and the unconnected crystals are known as B (bridged tetrahedra) [17]. The C-S-H internal product in relatively large C3S or alite grains appears to consist of small spherical particles, 4–8 nm in size in hydrated pastes at 20 °C, but smaller at higher temperatures, in the range of 3–4 μm [19].

Research has shown that high temperatures have a negative effect on the microstructure of concrete [20-25]. As the temperature increases, the porosity in the microstructure of concrete increases [26]. Heat causes water to evaporate and escape from the concrete mixture, disrupting and weakening the polymerization process and causing damage to various parts of the concrete microstructure. Research has shown that due to the high interstitial pressure, water escapes from the chemical bond space in hydrated calcium silicate gel (as the main product of the polymerization process) leads to concrete failure at temperatures above 450 ℃ [27]. The use of additives with pozzolanic properties in the concrete mixture can improve the production of hydrated gels in concrete [1-5,28]. In this regard, research has shown that the use of nanoparticles with pozzolanic properties can improve the mechanical and microstructural properties of concrete exposed to high temperatures [3-5,28]. The type of materials used in concrete, such as aggregates, has a significant impact on improving the resistance of concrete to high temperatures [30]. In this regard, research has shown that the use of sea sand in the concrete mixture, due to its high mechanical and chemical properties in its microstructure, can make the resulting concrete more resistant to high temperatures (compared to the use of natural sand) [31]. Research has shown that when high temperatures are applied to concrete, the amount of pores in the concrete increases due to the increase in internal vapor pressure [32]. This factor plays an effective role in reducing the mechanical properties and durability of heated concrete. The reduction in the resistance of concrete under heat is mainly attributed to the decomposition of calcium hydroxide, and this phenomenon usually occurs in the temperature range between 450 and 500 ℃ [33]. Hertz has reported that the C-S-H gel structure decomposes at 600 °C and is destroyed at 800 ℃ [34]. The

occurrence of these processes causes a decrease in the resistance of concrete to applied loads and the permeability of concrete in corrosive environments. Other studies show that high temperatures (in the range of 600 ℃) cause a decrease in the modulus of elasticity in concrete [4,5,20,28,35]. Also, the destructive effects of high temperatures (in the range of 600 ℃) on the chemical composition of hardened concrete have been reported according to the results of XRD analysis [3,4,36-38]. Microstructural studies obtained from SEM analysis show that high temperatures (in the range of 600 ℃) cause great damage to the microstructure of concrete [3-5,20,37,39]. In this laboratory study, the investigation of the microstructural properties of ordinary concrete containing high grades of Portland cement is proposed as an innovative design with regard to the modulus of elasticity test and XRD and SEM analysis.

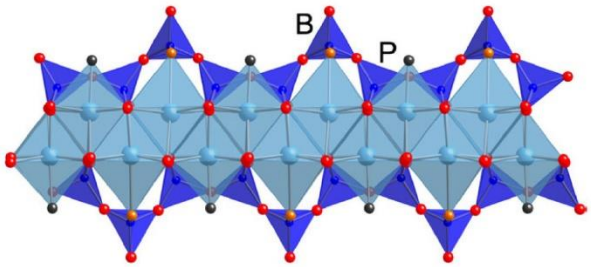

Fig. 1. Structure of C-S-H Gel [17]

2. Materials

The cement used in this laboratory study with a density of 3250 kg/m^3 and a specific surface area of 3100 cm3/g is Portland Type 2, produced by the Gilan Sabz Cement Industries Factory (Dilman), which is produced under the En 197-1 standard. Table 1 shows the chemical characteristics of the cement used. The water used to prepare lime water and make the mixture design in the current study is from the drinking water of Lahijan city. This water has a pH in the range of 5.6 to 5.7 and a density of 1000 kg/m^3. According to Section 9-10-4-2 and 9-10-4-3 of the fourth edition of the National Building Regulations of Iran, water that is drinkable, has no distinct taste or odor, and is clean and clear can be used in concrete without testing, unless previous records indicate that this water is unsuitable for concrete. The aggregate grading curve used is in accordance with Figure 2 within the ASTM C33 standard. The aggregates used were supplied from sand and gravel factories in Lahijan and were cleaned to remove organic impurities. Some of the characteristics of the fine and coarse aggregates used in this study within the aforementioned standard range have been determined based on Table 2. The superplasticizer used in this study is a fourth-generation normal polycarboxylate-based product from Durochem Middle East Company under the trade name Flowcem R700. This material was used in ordinary concrete to compensate for the poor performance and maintain the fluidity of the mortar mixture due to the high grade of Portland cement used. Some of the characteristics of the normal polycarboxylate superplasticizer are presented in Table 3.

Table 1.
Chemical Characteristics of Type II Portland Cement

Existing Material	%
Cl	Max 0/003
SiO2	21-22
Al2O3	4.5-4.8
Fe2O3	3.5-3.8
Cao	42-43
MgO	Max1.45
SO3	2-2.3
Na2O+0.658K2O	MAX 0.6
I.R	MAX 0/7
C3A	5.5-7.5
L.O.I	MAX 1/5

Table 2.
Specifications of Aggregate Used

Concrete Aggregates	Gravel	Sand
Minimum Diameter	4.75 (mm)	75 (µm)
Maximum Diameter (mm)	19	4.75
Modulus of Elasticity (mm)	5.7	2.85
Density (kg/m^3)	2750	2650
Water Absorption (%)	2.2	2.9

Table 3.
Superplasticizer Characteristics

Chemical Formula	Normal Polycarboxylate
Physical Condition	Liquid
Color	Light Brown
Density (kg/m^3)	1100
Consumption Standard	ASTM C494
pH	About 7

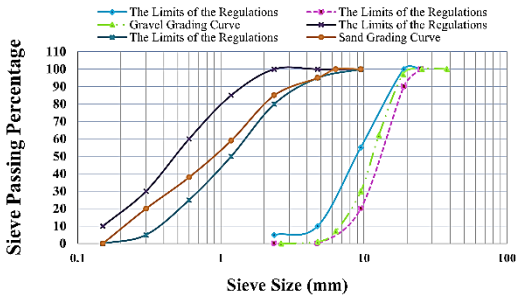

Fig. 2. Aggregate Curve

3. Mix Design and Curing

The conventional concrete mix design in this study was prepared based on the proposal of the American Concrete Association under the recommendation of the ACI Committee 211.1-89 [40], in accordance with Table 4. In this regard, the density of conventional concrete was determined to be 2397.9 kg/m^3 and the water-to-cement ratio was determined to be 0.45. In this regard, first, dry

materials were poured into the rotating mixer and the mixing process lasted for 1.5 minutes, then water and superplasticizer were added to the mixture and the mixing of the materials lasted for another 2 minutes. Next, the concrete molds that had been previously foiled and oiled were filled with concrete in three stages and in each stage, 25 blows were applied to the concrete with a special rod to compact the concrete components. After concreting, the samples were kept in a dry environment at a temperature of 21 ℃ for 24 hours and after demolding, they were kept and cured in lime water at a temperature of 21 ℃ until the test time. In preparing the mixture design in this study, the percentages determined for material consumption were selected based on standards (regarding mixture design and materials used) and the study and review of laboratory research by other researchers on the subject of this study.

Table 4.
Concrete Mix Design Specifications

Materials	Density (kg/m^3)	C.W (kg/m^3)	C.W* (%)	Control Number**
Cement	3250	500	20.85	0.1547
Water	1000	225	9.38	0.225
Gravel	2750	1000	41.7	0.3636
Sand	2650	666.15	27.78	0.2513
PNS***	1100	6.75	0.0028	0.006

* Consumed Weight
** The control number is the result of dividing the weight used by the density, and the sum of the numbers of each design must be 1 (taking into account an error coefficient of up to 3%).
*** Polycarboxylate Normal Superplasticizer

In this regard, the weight of cement used was selected as 500 kg/m^3, and by determining the water to cement ratio (0.45), the weight of water was also determined, the weight of sand in the mixture design was considered constant (1000 kg/m^3 of concrete mixture), and the consumption of superplasticizer was also determined within the range of 0.013 of the weight of cement used, and the amount of sand was also calculated and determined as a variable based on the relationships. In this study, superplasticizer was used in order to increase the efficiency of ordinary concrete due to the high grade of Portland cement and the low percentage of water to cement (0.45). In this regard, the amount of superplasticizer added to ordinary concrete was determined to be such that the slump in ordinary concrete could meet the requirements of the Iranian National Standard Nos. 2930, 6044, and 3203. Also, considering that the concrete produced was not of the air-entraining type, no air-entraining bubble additives were used in the concrete. In this laboratory study, 10 concrete samples were made, of which 6 concrete samples with cylindrical dimensions of 30×15 cm were made to perform elastic modulus testing under ambient temperature (3 samples) and high temperature (3 samples), 2 concrete samples with cubic dimensions of 10×10×10 cm were made to perform SEM analysis under ambient temperature (1 sample) and high temperature (1 sample), and 2 concrete samples with cubic dimensions of 10×10×10 cm were made to perform XRD analysis under ambient temperature (1 sample) and high temperature (1 sample).

4. Standards and Test Methods

The modulus of elasticity test was performed on cylindrical samples with dimensions of 30×15 cm after the concrete was stored in the lime water basin and after 90 days of this process (concrete curing conditions), at room temperature and under 600 ℃ (room temperature and high temperature are the test conditions), in accordance with the ASTM C469 standard [41]. In this regard, the desired sample was placed inside the concrete modulus of elasticity test frame, then the concrete sample with a cross section of 15 cm was placed vertically between the two plates of the concrete breaking jack device, then a load was applied at a speed between 0.5 and 0.9 kN/s until the sample deformed on its vertical axis. The longitudinal deformation of the concrete sample was measured using a gauge or strain gauge attached to the frame. XRD analysis was performed after 90 days of curing at room temperature and under high temperature according to BS EN 13925 [42] using a Philips PW1730 X-ray diffraction spectrometer. In this regard, crushed samples taken from the center of the concrete sample were placed inside the device and during the test, a diffraction diagram of the concrete crystals was prepared. The data obtained from X-ray diffraction is in the form of photon intensity depending on the detector angle 2θ, which is presented as a list of peak locations and their intensities on the graphs. SEM analysis was performed after 90 days of curing at room temperature and under high temperature according to ASTM C1723 [43] using a FEI Quanta200 scanning electron microscope. In this regard, the crushed concrete sample was placed in the device and images were recorded at the desired magnification and then microstructurally examined. Before performing the high-temperature tests, which were performed after a curing age of 90 days, according to the ISO834 standard [44], the concrete samples were placed in a furnace at a temperature of 600 °C for 1 hour, then the samples remained in the furnace for another 1 hour to avoid the effect of thermal shock. After the samples were removed from the furnace, the samples were kept at room temperature for 24 hours to reach temperature equilibrium. The use of this standard in other research on high-temperature tests in concrete has been reported [1,6,45].

5. Test Results and Interpretation

5.1. Elastic Modulus Test Results

The results of the elastic modulus test of concrete after a curing age of 90 days at 21 °C and after applying heat to 600 °C are shown in the graph in Figure 3. The results of each test are the average of the results of three laboratory samples. Based on these results, the elastic modulus at 21 °C and high heat was obtained as 33.73 and 12.24 GPa, respectively, which shows a 63.71% decrease in the elastic modulus after applying high heat to the concrete. Studies show that heat causes water to evaporate from the pores and cavities in the microstructure matrix of concrete, and with increasing porosity and the creation of microcracks in the concrete, the elastic modulus in the concrete will decrease. Evaporation of water from the concrete structure is always accompanied by a loss of weight, which can cause thermal cracks due to shrinkage. Research has shown that the rate of acquisition of elastic modulus of concrete increases rapidly at early ages [46-49]. In this regard, increasing the curing age (in this paper up to 90 days) of concrete has improved the result of elastic modulus in concrete under 21 °C and after applying high heat. This is due to the role of high cement grade consumption in increasing the strength of hardened concrete and the progress of the polymerization process with increasing curing age. Under these conditions, with greater participation of cement particles in the polymerization process, the volume of C-A-S-H and C-S-H gels, which are the final product of the chemical process between water and cementitious materials, increases. The main role of these gels in the composition of concrete is to fill the capillary pores, cavities and cracks in the structure of the cement matrix, on the other hand, it covers the connection in the interfacial transition zones (ITZ) at the aggregate interface. The results of XRD and SEM analysis in this study provide an interpretation of the effective role of C-S-H gel in the polymerization process and changes in concrete under high temperature. Other studies have shown that high temperatures (in the range of 600 °C) cause a decrease in the modulus of elasticity in concrete [20,28,35]. Figure 4 shows a concrete sample undergoing a modulus of elasticity test, in which the deformation of the concrete (due to changes in the gauge attached to the concrete sample) under force application is visible.

5.2. XRD Analysis Results

In this laboratory study, X-ray diffraction (XRD) spectroscopy was used to study and analyze the crystalline structure of the materials and to investigate the presence of grains and particles in the concrete. The results of the XRD analysis after a curing age of 90 days at 21 and 600 °C are shown in Figure 5.

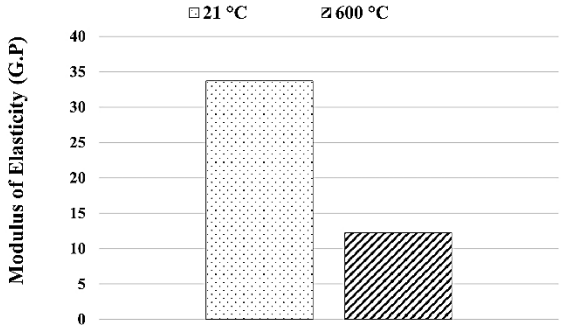

Fig. 3. Concrete Modulus of Elasticity Test Results

Fig. 4. Concrete Deformation in the Modulus of Elasticity Test

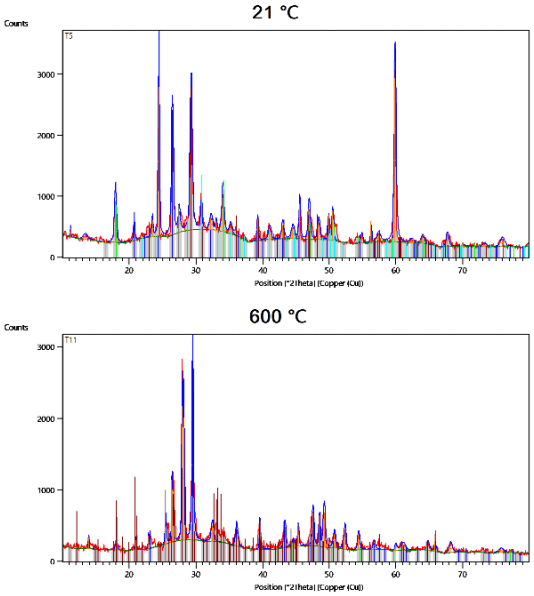

Fig. 5. XRD Test Results

Figure 6 shows a sample image of the XRD device. Based on these results, it is observed that at a temperature of 21 °C, aluminum phosphate compounds with a maximum peak height of 2670 at an angle of 59.85 degrees, followed by calcium hydroxide with a maximum peak

height of 2452 at an angle of 24.41 degrees, titanium oxide with a maximum peak height of 1794 at an angle of 29.24 degrees, calcite with a maximum peak height of 1600 at an angle of 26.45 degrees, and dolomite with a maximum peak height of 671 at an angle of 17.92 degrees, have the highest dispersion. After the removal of some elements in the high-temperature calcination process, compounds such as calcium manganese carbonate with a maximum peak height of 2092 at an angle of 29.47 degrees, carbon with a maximum peak height of 1865 at an angle of 27.9 degrees, hydrated aluminum manganese iron potassium silicate with a maximum peak height of 1712 at an angle of 28.13 degrees, and hydrated calcium aluminum silicate with a maximum peak height of 726 at an angle of 26.42 degrees have the highest dispersion.

Fig. 6. XRD Device

Applying high temperature to concrete samples has reduced the height of the peaks due to the presence of hydrated compounds, this has also been observed in the research of others [3,4], in this regard, the difference in the peak height in the XRD graph at a temperature of 21 °C (with a height of 2092) compared to a temperature of 600 °C (with a height of 2670) is 21.64%. Studies show that under the effect of high temperature in concrete, CH gel does not convert into calcium carbonates such as Calcite and as is clear from the results of the table, CH disappears at high temperature and is actually converted into Carbon and C-A and this is the main cause of the weakness of concrete at high temperature [50,51]. In other research, the destructive effects of high temperature (in the range of 600 °C) on the chemical composition of hardened concrete have been reported according to the results of XRD tests [36-38].

5.3. SEM Analysis Results

The results of the analysis of scanning electron microscope images with a scale of 3 and 20 µm under temperatures of 21 and 600 °C after a curing age of 90 days in the concrete from the current research are shown in Figure 7. Figure 8 shows an example of the SEM device. According to the images, it is observed that the microstructure of concrete consists of three basic separate and different phases as follows [1-5]:

1. The first phase includes the polymerization products containing hydrated C-A-S-H and C-S-H gels, which are mainly dark in the images, in this regard, the C-S-H gel has formed the largest volume of the cement paste.
2. The second phase includes unreacted crystals, which are a result of impurities in the raw materials or unreacted particles in the polymerization process, and are mainly white in SEM images.
3. The third phase includes the way the cement paste bonds with the aggregate in the ITZ.

In the images taken at a temperature of 21 °C, the volume of C-A-S-H and C-S-H gels is seen in a high amount in the mixture, which indicates high quality and density in the concrete, and this is mainly due to the completion of a large part of the polymerization process after the age of 90 days of curing and the use of high cement grade in the concrete mixture. The amount of pores and cracks is seen in a minimum amount in the images. White spots are caused by unhydrated cement particles and Ca(OH)2 not participating in the chemical process, in this regard, finer particles are often related to unhydrated cement particles and coarser particles to Ca(OH)2. Studies have shown that the presence of C-A-S-H crystals in the concrete composition formed due to the chemical weakness of concrete in the vicinity of sulfate environments and Ca(OH)2 crystals formed due to the weakness of concrete in the vicinity of acidic environments can have an adverse effect on the mechanical properties and durability of concrete. The images indicate that applying high heat to the concrete sample has caused damage to the microstructure of the concrete due to the water escaping from the pores and capillary pores. Accordingly, it is observed that the volume of porous areas and tree-shaped structure resulting from the destruction of the concrete matrix under high heat are present in large quantities. The size of the pores in the heated sample is much larger than that of the sample placed at 21 °C. On the other hand, due to the damage to the concrete microstructure, the volume of hydrated C-A-S-H and C-S-H gels in the mixture has been reduced. These factors are the main reasons for the decrease in the results observed in the heated concrete compared to the concrete exposed to ambient temperature in the elastic modulus and XRD tests in this study. Microstructural studies obtained from SEM analysis show that high heat (in the range of 600 °C) causes great damage to the microstructure of the concrete [20,37,39]. The presence of Ca(OH)2 particles in the

images indicates that a major part of this hydrated material has not been able to fully participate in the chemical process, and this could be due to the high cement content in the concrete, which increased the polymerization rate and did not give the opportunity for the chemical participation of some cementitious materials. Studies have shown [4,5,7] that after the materials used in the preparation and manufacture of concrete are combined, the process of chemical reaction (polymerization) between cementitious materials and water begins. The speed and extent of formation of hydrated gels, which are the final product of the chemical composition in concrete, mainly depends on the properties and ratios of cementitious materials and water.

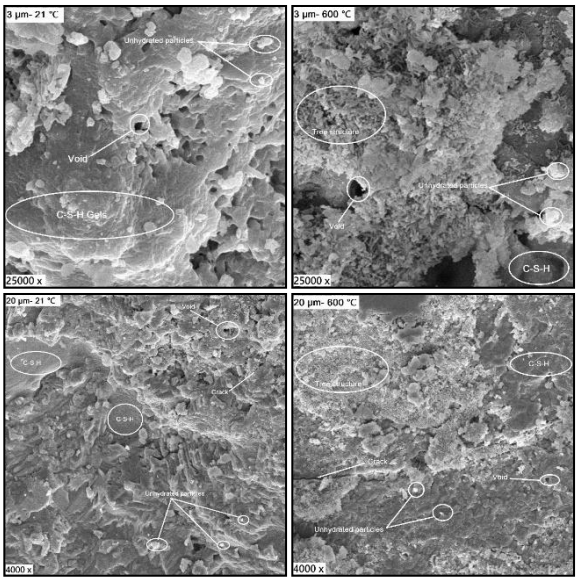

Fig. 7. SEM Images

Fig. 8. SEM Device

6. Conclusion

In this laboratory study, the microstructure of ordinary concrete containing Portland cement with a grade of 500 kg/m3 at a temperature of 21 °C and high heat (600 ℃) was evaluated. In this regard, elastic modulus test and XRD and SEM analysis were performed on concrete samples. The results of this study are presented as follows.

1. In the elastic modulus test, applying heat to the concrete sample caused a decrease in the result. So that the elastic modulus of concrete decreased from 33.73 to 12.24 GPa, which resulted in a decrease of 63.71%. Similar results have also been obtained in the study of others [4].
2. In the XRD test at 21 °C, aluminum phosphate compounds with a maximum peak height of 2670 at an angle of 59.85 degrees, followed by calcium hydroxide with a maximum peak height of 2452 at an angle of 24.41 degrees, titanium oxide with a maximum peak height of 1794 at an angle of 29.24 degrees, calcite with a maximum peak height of 1600 at an angle of 26.45 degrees, and dolomite with a maximum peak height of 671 at an angle of 17.92 degrees, have the highest dispersion.
3. In the XRD test at 600 °C, compounds such as calcium manganese carbonate with a maximum peak height of 2092 at an angle of 29.47 degrees, carbon with a maximum peak height of 1865 at an angle of 27.9 degrees, hydrated aluminum manganese iron potassium silicate with a maximum peak height of 1712 at an angle of 28.13 degrees and hydrated aluminum calcium silicate with a maximum peak height of 726 and at an angle of 26.42 degrees have the highest dispersion. In this regard, the decrease in the height of the presence of elements under heat compared to the spectrum of concrete at 21 °C is evident.
4. The presence of Ca(OH)2 crystals with a high peak height in the X-ray diffraction spectrum at 21 °C is due to the incomplete polymerization process in the ordinary cement matrix. The low age of the curing period increases the volume of these crystals in the concrete mixture, which decreases with the age of the concrete. The high grade of cement used in the concrete mixture can intensify the presence of Ca(OH)2 crystals by accelerating the polymerization process. Similar results have also been obtained in the research of others [3].
5. In SEM images at a temperature of 21 °C, the volume of hydrated gels is seen in high amounts. This is due to the use of high grade of cement in

the mixture and the completion of a large part of the polymerization process, which has led to a reduction in the size and number of pores and cracks in the matrix structure of ordinary concrete. Similar results have also been obtained in the research of others [1,2,7].

6. Applying heat of 600 °C to concrete samples has caused water to be removed and microstructural phases in concrete to be destroyed. In this regard, the creation of a tree structure, destruction of the hydrated gel structure and an increase in the number and size of pores are evident in SEM images. Similar results have been obtained in the research of others [3,4,5].
7. Evaluation of SEM images of the microstructure of concrete at temperatures of 21 and 600 °C was in agreement and overlap with the results obtained from the elastic modulus test and XRD analysis.

References

[1] Mansourghanaei, Mohammadhossein, Morteza Biklaryan, and Alireza Mardookhpour. "Durability and mechanical properties of granulated blast furnace slag based geopolymer concrete containing polyolefin fibers and nano silica." KSCE Journal of Civil Engineering 28.1 (2024): 209-219. https://doi.org/10.1007/s12205-023-2202-6

[2] Mansourghanaei, Mohammadhossein, Morteza Biklaryan, and Alireza Mardookhpour. "Experimental study of the effects of adding silica nanoparticles on the durability of geopolymer concrete." Australian Journal of Civil Engineering 22.1 (2024): 81-93. https://doi.org/10.1080/14488353.2022.2120247

[3] Mansourghanaei, Mohammadhossein, Morteza Biklaryan, and Alireza Mardookhpour. "Experimental study of properties of green concrete based on geopolymer materials under high temperature." Civil Engineering Infrastructures Journal 56.2 (2023): 365-379. https://doi.org/10.22059/ceij.2022.345402.1856

[4] Mansourghanaei, Mohammadhossein, and Alireza Mardookhpour. "Analysis of the Numerical Results Obtained from the Experimental Examination of the Mechanical Properties of Geopolymer Concrete." Numerical Methods in Civil Engineering 9.1 (2024): 31-41. https://doi.org/10.61186/NMCE.2402.1047

[5] Mansourghanaei, Mohammadhossein, Morteza Biklaryan, and Alireza Mardookhpour. "Experimental Study of Mechanical Properties of Slag Geopolymer Concrete under High Temperature, Used in Road Pavement." International Journal of Transportation Engineering 11.1 (2023): 1371-1385.

[6] Mansourghanaei, Mohammadhossein, and Alireza Mardookhpour. "Investigating the Properties of Environmentally Friendly Green Concrete (Geopolymer) Under High Temperature." Sustainable Earth Trends 3.4 (2023): 62-69. https://doi.org/10.48308/ser.2024.234846.1038

[7] Mansourghanaei, Mohammadhossein, Morteza Biklaryan, and Alireza Mardookhpour. "Experimental study of modulus of elasticity, capillary absorption of water and UPV in nature-friendly concrete based on geopolymer materials." International Journal of Advanced Structural Engineering 12.2 (2022): 607-615.

[8] Mansourghanaei, Mohammadhossein. "Experimental Evaluation of The Impact Resistance of Alkali-Activated Slag Concrete Under High Temperature." Journal of Civil Engineering Researchers 6.3 (2024): 47-53. https://doi.org/10.61186/JCER.6.3.47

[9] Mansourghanaei, Mohammadhossein. "Investigating the Mechanical and Durability Properties of Geopolymer Concrete Based on Granulated Blast Furnace Slag as Green Concrete." Journal of Civil Engineering Researchers 5.3 (2023): 24-34. https://doi.org/10.61186/JCER.5.3.24

[10] Mansourghanaei, Mohammadhossein. "Evaluation of Mechanical Properties and Microstructure of Pozzolanic Geopolymer Concrete Reinforced with Polymer Fiber." Journal of Civil Engineering Researchers 5.2 (2023): 1-13. https://doi.org/10.61186/JCER.5.2.1

[11] Tadaion, M., Hani Honarmand, and Moosa Kalhori. "Impact of Plasticizers on The Quality of Concrete and The Reduction of the Cement Content." Concrete Research 3.2 (2010): 49-57.

[12] Naderi, Mahmood, Rezvan Valibeigi, and Seyed Mohammad Mirsafi. "Studying the Effects kind of Curing on Strengths and Permeability of Concrete." Journal of Structural and Construction Engineering 5.3 (2018): 106-123. https://doi.org/10.22065/jsce.2017.69343.1013

[13] Kazemian, Sina, and S. Ghareh. "Effects of Cement, Different Bentonite, and Aggregates on Plastic Concrete in Besh-Ghardash Dam, Iran." Journal of Testing and Evaluation 45.1 (2017): 242-248. https://doi.org/10.1520/JTE20160161

[14] Mehta, Povindar K., and Paulo Monteiro. "Concrete: microstructure, properties, and materials." McGraw-Hill Education (2014).

[15] Lin, Weihui, et al. "Dynamic mechanical behaviors of calcium silicate hydrate under shock compression loading using molecular dynamics simulation." Journal of Non-Crystalline Solids 500 (2018): 482-486. https://doi.org/10.1016/j.jnoncrysol.2018.09.007

[16] Juenger, M. C. G., et al. "Advances in alternative cementitious binders." Cement and concrete research41.12 (2011): 1232-1243. https://doi.org/10.1016/j.cemconres.2010.11.012

[17] Richardson, Ian G. "The calcium silicate hydrates." Cement and concrete research 38.2 (2008): 137-158. https://doi.org/10.1016/j.cemconres.2007.11.005

[18] Taylor, H. F. W. "Hydration of Cements." Proc. Fifth Int. Symp. on the Chemistry of Cement.. 1968.

[19] Richardson, I. G. "Tobermorite/jennite-and tobermorite/calcium hydroxide-based models for the structure of CSH: applicability to hardened pastes of tricalcium silicate, β-dicalcium silicate, Portland cement, and blends of Portland cement with blast-furnace slag, metakaolin, or silica fume." Cement and concrete research 34.9 (2004): 1733-1777. https://doi.org/10.1016/j.cemconres.2004.05.034

[20] Tayeh, Bassam A., et al. "Effect of air agent on mechanical properties and microstructure of lightweight geopolymer concrete under high temperature." Case studies in construction materials 16 (2022): e00951. https://doi.org/10.1016/j.cscm.2022.e00951

[21] Li, Yang, et al. "Influence of different alkali sulfates on the shrinkage, hydration, pore structure, fractal dimension and microstructure of low-heat Portland cement, medium-heat Portland cement and ordinary Portland cement." Fractal and Fractional 5.03 (2021): 79. https://doi.org/10.3390/fractalfract5030079

[22] Li, Shuangxin, et al. "Effects of isothermal microwave heating on the strength and microstructure of ultra-high performance concrete embedded with steel fibers." Journal of Materials Research and Technology 14 (2021): 1893-1902. https://doi.org/10.1016/j.jmrt.2021.07.092

[23] Amin, Mohamed, et al. "Effect of high temperatures on mechanical, radiation attenuation and microstructure properties of heavyweight geopolymer concrete." Structural Engineering and Mechanics, An Int'l Journal80.2 (2021): 181-199.

[24] Malik, Manisha, S. K. Bhattacharyya, and Sudhirkumar V. Barai. "Microstructural changes in concrete: Postfire scenario." Journal of

Materials in Civil Engineering 33.2 (2021): 04020462. https://doi.org/10.1061/(ASCE)MT.1943-5533.0003449
[25] Yu, Baoying, et al. "Compressive strength development and microstructure of magnesium phosphate cement concrete." Construction and Building Materials 283 (2021): 122585. https://doi.org/10.1016/j.conbuildmat.2021.122585
[26] Akçaözoğlu, Semiha, et al. "Examination of mechanical properties and microstructure of alkali activated slag and slag-metakaolin blends exposed to high temperatures." Structural Concrete 23.2 (2022): 1273-1289. https://doi.org/10.1002/suco.202000080
[27] Siddique, Rafat, and Deepinder Kaur. "Properties of concrete containing ground granulated blast furnace slag (GGBFS) at elevated temperatures." Journal of Advanced Research 3.1 (2012): 45-51. https://doi.org/10.1016/j.jare.2011.03.004
[28] Tobbala, D. E., et al. "Performance and microstructure analysis of high-strength concrete incorporated with nanoparticles subjected to high temperatures and actual fires." Archives of Civil and Mechanical Engineering 22.2 (2022): 85. https://doi.org/10.1007/s43452-022-00397-6
[29] Althoey, Fadi, et al. "Performance of cement mortars containing clay exposed to high temperature." Arabian Journal for Science and Engineering (2022): 1-9. https://doi.org/10.1007/s13369-021-05583-x
[30] Wang, Hui, et al. "Thermal stresses in rectangular concrete beams, resulting from constraints at microstructure, cross-section, and supports." European Journal of Mechanics-A/Solids 93 (2022): 104495. https://doi.org/10.1016/j.euromechsol.2021.104495
[31] Vafaei, Davoud, et al. "Microstructural and mechanical properties of fiber-reinforced seawater sea-sand concrete under elevated temperatures." Journal of Building Engineering 50 (2022): 104140. https://doi.org/10.1016/j.jobe.2022.104140
[32] Abolhasani, Amirmohamad, et al. "A comprehensive evaluation of fracture toughness, fracture energy, flexural strength and microstructure of calcium aluminate cement concrete exposed to high temperatures." Engineering Fracture Mechanics 261 (2022): 108221. https://doi.org/10.1016/j.engfracmech.2021.108221
[33] Bentz, Dale P. "Fibers, percolation, and spalling of high-performance concrete." Materials Journal 97.3 (2000): 351-359.
[34] Hertz, Kristian Dahl. "Concrete strength for fire safety design." Magazine of concrete research 57.8 (2005): 445-453. https://doi.org/10.1680/macr.2005.57.8.445
[35] Fan, Kunjie, et al. "Compressive stress-strain relationship for stressed concrete at high temperatures." Fire Safety Journal 130 (2022): 103576. https://doi.org/10.1016/j.firesaf.2022.103576
[36] Liu, Chihao, and Jiajian Chen. "High temperature degradation mechanism of concrete with plastering layer." Materials 15.2 (2022): 398. https://doi.org/10.3390/ma15020398
[37] Dash, Manoj K., et al. "Impact of elevated temperature on strength and micro-structural properties of concrete containing water-cooled ferrochrome slag as fine aggregate." Construction and Building Materials 323 (2022): 126542. https://doi.org/10.1016/j.conbuildmat.2022.126542
[38] Mostafa, Sahar A., et al. "Experimental study and theoretical prediction of mechanical properties of ultra-high-performance concrete incorporated with nanorice husk ash burning at different temperature treatments." Environmental Science and Pollution Research 29.50 (2022): 75380-75401. https://doi.org/10.1007/s11356-022-20779-w
[39] Hasan-Ghasemi, Ali, Mahdi Nematzadeh, and Hossein Fallahnejad. "Post-fire residual fracture characteristics and brittleness of self-compacting concrete containing waste PET flakes: experimental and theoretical investigation." Engineering Fracture Mechanics 261 (2022): 108263. https://doi.org/10.1016/j.engfracmech.2022.108263
[40] ACI Committee. "Standard practice for selecting proportions for normal, heavyweight, and mass concrete." Pub. L. No. ACI 211 (2002): 121.
[41] ASTM C469 /C469M-14, "Standard Test Method for Static Modulus of Elasticity and Poisson's Ratio of Concrete in Compression," ASTM International, 2014.
[42] Berti, Giovanni. "EN 13925-1 Non-destructive testing-X-ray diffraction from polycrystalline and amorphous material-Part 1: General principles." (2008): 1-13.
[43] ASTM C1723-16. "Standard guide for examination of hardened concrete using scanning electron microscopy." Annual book of ASTM standards (2016).
[44] ISO, ISO. "834-1: 1999-Fire-resistance tests—elements of building construction–part 1: general requirements." Int Organ Stand (1999).
[45] Kong, Daniel LY, and Jay G. Sanjayan. "Effect of elevated temperatures on geopolymer paste, mortar and concrete." Cement and concrete research 40.2 (2010): 334-339. https://doi.org/10.1016/j.cemconres.2009.10.017
[46] Abd Elaty, Metwally Abd Allah. "Compressive strength prediction of Portland cement concrete with age using a new model." HBRC journal 10.2 (2014): 145-155. https://doi.org/10.1016/j.hbrcj.2013.09.005
[47] Kim, J-K., Y-H. Moon, and S-H. Eo. "Compressive strength development of concrete with different curing time and temperature." Cement and Concrete Research 28.12 (1998): 1761-1773. https://doi.org/10.1016/S0008-8846(98)00164-1
[48] Madandoust, Rahmat, John H. Bungey, and Reza Ghavidel. "Prediction of the concrete compressive strength by means of core testing using GMDH-type neural network and ANFIS models." Computational Materials Science 51.1 (2012): 261-272. https://doi.org/10.1016/j.commatsci.2011.07.053
[49] Pirmohammadi Alishah, Farhad, and Navid Mahmoudzadeh. "Investigation of the effect of bentonite paste index on modulus of elasticity, compressive strength and performance of plastic concrete." Civil and Project 2.5 (2020): 87-109.
[50] Rashad, Alaa M. "The effect of polypropylene, polyvinyl-alcohol, carbon and glass fibres on geopolymers properties." Materials Science and Technology 35.2 (2019): 127-146. https://doi.org/10.1080/02670836.2018.1514096
[51] Morsy, M. S., et al. "Behavior of blended cement mortars containing nano-metakaolin at elevated temperatures." Construction and Building materials 35 (2012): 900-905. https://doi.org/10.1016/j.conbuildmat.2012.04.099